A Joint DLR-ONERA Contribution to CFD-based Investigations of Unconventional Empennages for Future Civil Transport Aircraft

Gérald CARRIER[1] and Lutz GEBHARDT[2]
[1] ONERA, Applied Aerodynamics Department
BP72, 92322 Châtillon Cedex, France, e-mail: gerald.carrier@onera.fr
[2] DLR, Institute of Aerodynamics and Flow Technology
D-38108 Braunschweig, Germany, e-mail: lutz.gebhardt@dlr.de

Summary

The introduction of innovative empennage configurations on transonic transport aircraft may potentially improve their aerodynamic performance due to a reduction of the wetted surface and a corresponding decrease in drag. This paper describes the CFD analysis performed at DLR and ONERA in the context of the European research project NEFA to investigate some key aerodynamics features related to alternative tail configurations. Emphasis is placed on the aerodynamic performance at cruise flight conditions of three tail variants of an otherwise identical aircraft: a conventional tail, a U-tail and a V-tail empennage. The results obtained confirm the potential aerodynamic benefits of the V-tail configuration and show that the U-tail has about the same performance as the conventional tail.

1 Introduction

To satisfy stability, controllability and handling qualities requirements, conventional aircraft designs include empennage-mounted tail surfaces. With current transport aircraft types, these tail surfaces consist of a combination of a vertical and a horizontal tail plane (VTP and HTP). This conventional tail configuration has the advantage of decoupling, to a large extent, the longitudinal and lateral effects of control surface deflections. However this layout is also responsible for a considerable part of the wetted area of the aircraft with corresponding friction drag, in addition to the interference drag resulting from the intersections of the three tail surfaces with the fuselage. Alternative tail configurations may potentially improve the aerodynamic performance of an aircraft while still maintaining an equivalent tail authority. In the case of the V-tail, the potential aerodynamic benefits are the result of a reduction in wetted surface area and in interference drag (only two instead of three tail surfaces have to be mounted on the fuselage). The drag reduction potential of the U-tail is not likely to be very high as a large reduction in wetted area does not seem possible. On the other hand, interference drag may be lower due to the reduced number of

intersections with the fuselage. As the U-tail offers benefits from a noise shielding perspective for aft mounted engines, it may be a worthwhile alternative to a conventional tail if it does not incur a noticeable drag penalty in comparison.

The objective of this paper is to analyse the potential benefits that can be offered by V- and U-tail configurations in terms of aerodynamic performance at cruise flight conditions compared to a conventional tail concept. For this purpose, three aircraft tail geometries are investigated and compared, respectively a reference tail (conventional vertical and horizontal tail planes), a V-tail and a U-tail. After introducing the European research project NEFA in which the work hereafter presented has been carried out, the numerical methods applied in these investigations are briefly described. Lift and drag characteristics are first compared and evaluated, followed by a section with special emphasis on the analysis of the V-tail design for which trim drag development is investigated and the aerodynamic performance at cruise flight condition is compared with the reference tail design.

2 The European Research Project NEFA

The ongoing European research project "New Empennage For Aircraft" (NEFA) has been set up to study the overall impact of new empennage concepts on the performance and handling qualities of a transport aircraft. In this project, V- and U-tail layouts are investigated that may provide performance and other improvements over conventional tails used today and thereby contribute to achieving the goals defined in the European Vision 2020 (reduction of fuel consumption by 50%, NOx by 80% etc…). Because alternative tail concepts will have a wide-ranging impact on many aspects of the aircraft, the multi-disciplinary trade-off between aerodynamics, structural weight changes, and handling qualities issues are investigated in the NEFA project.

The aerodynamic work package of NEFA (WP2) is intended to provide accurate evaluations of the tail configuration effect on the aerodynamic performance and on the handling qualities of the aircraft, and to give insight into the flow phenomena occurring with these unconventional tail designs for specific operating conditions. Within this work-package, ONERA and DLR are applying their expertise in aerodynamics and CFD to support the evaluation of the impact of new empennage types on the aircraft aerodynamics, together with other partners from several European countries: Airbus in France, Spain and Germany, Helsinki University of Technology (HUT) in Finland, Instituto Nacional de Tecnica Aeroespacial (INTA) in Spain and the Technical University of Braunschweig (TUBS) in Germany.

3 Aircraft Configuration, Tail Design and Flight Conditions

Starting from a conventional short-to-medium range transonic transport aircraft design representative of a 100-seat aircraft cruising at Mach number 0.77 and

equipped with a conventional horizontal and vertical tail (the reference tail), two alternative tail variants, respectively a V-tail and a U-tail were defined in the first work-package of the project. These tail configurations are the result of a multidisciplinary preliminary design optimization performed by the Future Projects Offices of Airbus in France with the constraint of yielding equivalent, certifiable handling qualities and taking several important design aspects like weight, handling qualities, aerodynamics, engine characteristics, mission profile etc. into account. This was followed by a refinement loop through detailed aerodynamic design work done at Airbus Germany in Bremen. The final V-tail design is a trimmable V-tail in combination with a modified empennage in the tail-to-fuselage junction area to account for the acute angle between tail and fuselage and the higher absolute thickness of the V-tail at the intersection with the fuselage. A graphical comparison of these configurations is depicted in Figure 1.

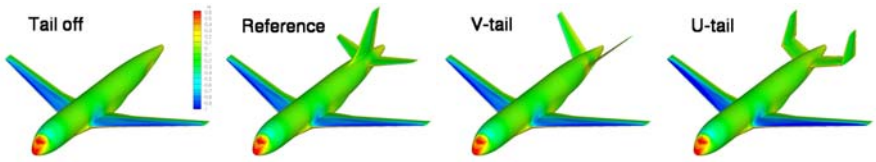

Figure 1: View of the 4 different tail configurations investigated. Pressure distributions from RANS calculations at M=0.77, C_L=0.4, Re=2.7*10^6.

All results presented in this paper correspond to the aircraft cruise flight conditions at a Mach number of 0.77 and a Reynolds number of 2.7 million as present in the high speed wind tunnel tests also performed as part of this project.

3 Methods

All aerodynamic investigations presented were carried out using the DLR TAU code [1]. TAU is a solver for the Reynolds-averaged Navier-Stokes equations for hybrid meshes. The Spalart-Allmaras one-equation turbulence model with Edwards modification was used for the investigations presented here.

The ONERA FFD70 drag post-processor, based on far-field analysis [2,3] has been applied to post-process the RANS solutions calculated with the TAU code. Compared to the commonly available near-field integration, this method has two main advantages: first, it yields a more accurate evaluation of the total aircraft drag and second, it provides a phenomenological drag breakdown into lift-induced, wave and viscous drag components.

4 Comparison of Reference-, U-, and V-tail Characteristics

A considerable part of the aerodynamic investigations in the NEFA project was devoted to the analysis of the tail characteristics by means of CFD. The emphasis of the DLR contribution was put on the cruise flight conditions (M=0.77) at wind

tunnel Reynolds numbers ($Re=2.7*10^6$). The computation results were then used to compare quantitatively lift and drag characteristics as well as tail efficiencies. Furthermore, flow phenomena were evaluated qualitatively by means of field and surface streamlines, c_p and c_f-distribution etc. As the more phenomenological analysis did not reveal any surprising effects, the part of the work presented here will focus on the quantitative results due to space limitations.

4.1 Computational Details

The calculation of tail polars and efficiencies requires a rather large number of computations at different tail incidence settings in combination with aircraft angle of attack and angle of sideslip. Therefore it was necessary to create hybrid meshes for the NS-solver TAU with a reasonable number of grid points, for which the commercial mesh generation package CENTAUR was used [4]. Because the mesh generation parameters were kept identical between the three configurations wherever possible in order to keep the solutions comparable, the number of grid points varies between 1.6 million for the tail-off configuration and 2.3 million for the U-tail configuration. The number of prism layers of the hybrid mesh is 25 on the lifting surfaces and 32 on the fuselage.

For symmetric onset flow conditions ($\beta=0°$), calculations at $\alpha \in \{-2°, 0°, 2°, 4°, 6°\}$ were performed for the tail-off configuration and in combination with three tail incidence settings $i_H \in \{-2°, 0°, 2°\}$. The surface pressure distribution calculated by TAU was integrated to obtain forces and moments using the DLR tool Aeroforce [5]. Because this tool allows an easy definition of split planes, data analysis could be done in a similar way to the Live Rear End (LRE) technique used in the wind tunnel investigations. A split plane is defined perpendicular to the fuselage axis between wing and tail, and the forces and moments of all parts behind the split plane are summed up. By subtracting the results from the calculations with and without tail, values for the isolated tail are obtained while taking installation effects and the downstream effect of wing and the forward part of the fuselage into account. Using the LRE method as described yields in a reduction of the rounding error as the numbers subtracted and their difference are of a similar order of magnitude which is not the case for the full aircraft with and without tail.

4.2 Determination of Downwash and Efficiency

In order to determine the tail plane efficiencies $\delta C_{LH}/\delta\alpha_H$, the mean downwash angle ε at the location of the tail must be computed first. ε can then be used to calculate α_H from α and i_H:

$$\alpha_H = \alpha - \varepsilon + i_H \tag{1}$$

This procedure assumes that lift, drag, moment and downwash change in a linear manner with α which means that the aircraft angles of attack α used and tail incidence settings i_H must be sufficiently small in order stay in the linear regime. Other phenomena which lead to non-linear behaviour like the occurrence of

shocks and/or separation must also be avoided. For the set of angles of attack computed in the course of these investigations, this was only perfectly true for $\alpha \in \{-2°, 0°, 2°\}$ for ref. tail and U-tail and for $\alpha \in \{-4°, -2°, 0°\}$ for the V-tail. This linear part of the polar was therefore used to determine the downwash angle. The distribution of C_{LH} vs. α resulting from Eq. (1) is plotted in Figure 2.

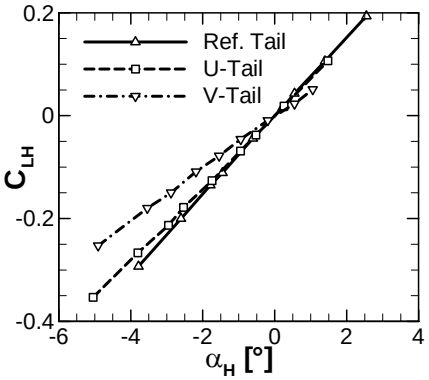

Figure 2: Comparison of the lift curve slope of the three tail configurations

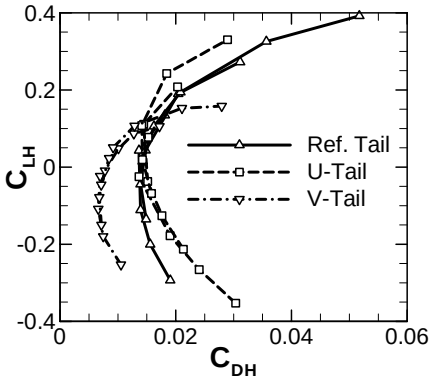

Figure 3: Tail drag polars for reference tail, U-tail and V-tail

The lift curve slope is usually taken as a measure for a tail's efficiency. In this regard, Figure 2 indicates that the reference tail has the highest efficiency, closely followed by the U-tail. This may be attributed partly to reduced aspect ratio of the U-tail HTP which does not seem to be completely offset by the two VTP's which act as winglets, i.e. increase the effective aspect ratio of the HTP part of the U-tail. When referencing the lift curve slope based on aircraft reference values, the two tails are almost identical in performance due to the smaller downwash coefficient of the U-tail in comparison to the reference tail. The V-tail efficiency on the other hand is noticeably lower, mainly due to the fact that the actual tail surface area is used as reference area for all configurations while only part of this area acts in the z- or lift direction due to the high dihedral angle of the V-tail (43.1°) in comparison to the other tail shapes (6°). Like in the case of the V-tail, this reduced efficiency or lift curve slope is partly offset by a lower downwash gradient, which can be attributed to the fact that a large part of the V-tail has a greater vertical distance from the wing wake position in the tail area.

4.3 Lift and Drag Characteristics

The dataset collected for the computation of the tail efficiencies can also be used to determine the tail drag polar. With C_{LH} already available, C_{DH} is calculated also using the LRE method. A set of computations at different α but identical i_H results in one "branch" of the drag polar. If several branches for different i_H are plotted in one diagram, one observes that the branches do not join each other. This is due to

different effective α_H for different i_H as a change in i_H also results in a change of the HTP position in the wing wake, which in turn results in a different downwash value at the tail. Therefore C_{LH} and C_{DH} must be corrected for ε as follows:

$$C_{LH,\alpha_H} = C_{LH,\alpha} \cdot \cos\varepsilon + C_{DH,\alpha} \cdot \sin\varepsilon \qquad (2)$$

$$C_{DH,\alpha_H} = C_{DH,\alpha} \cdot \cos\varepsilon - C_{LH,\alpha} \cdot \sin\varepsilon$$

Using values of ε determined from two successive calculation points, the branches for the different tail incidence settings join each other reasonably well (Figure 3).

Analysing the drag polars, some interesting conclusions can be drawn. First, reference tail and U-tail have similar minimum drag values, while C_{LH} for minimum drag is shifted to more positive C_{LH} values. Also, C_{DH} rises faster with increasing negative C_{LH}-value for the U-tail which is not as desirable as the behaviour of the reference tail. Keeping in mind that the design effort put into the U-tail configuration was considerably lower than for the reference or V-tail configuration, it seems likely that there is still some potential in the U-tail which could be used to adjust the shape of its drag polar. Even in the current state, the U-tail does not exhibit any negative characteristics from an aerodynamic point of view which would preclude its use on an actual aircraft configuration which might be desirable for example for noise shielding purposes in combination with aft mounted engines. It must be kept in mind though that the configuration investigated here does not have aft-mounted engines which could lead to increased drag due to mutual interference effects (compare for example [6]).

The drag polar of the V-tail clearly shows its distinct aerodynamic advantages in comparison to the two other tail shapes. It has a considerably lower minimum drag value at slightly negative C_{LH} values and very low drag variation between C_{LH}=0 and C_{LH}=-0.2. Drag rises faster for positive C_{LH} in relation to the reference tail, but up to about C_{LH}=+0.1 the drag of the V-tail is nevertheless lower than the one of the reference tail.

5 Trim Drag Analysis of the V-tail Configuration

To be able to trim the aircraft for different location of the centre of gravity (CG), the tail is used as a trimming surface which produces a lift and therefore a corresponding lift-induced drag contribution. For a conventional tail, the lift-induced drag due to trim is produced by the horizontal tail plane (HTP). With a relatively low dihedral angle, a conventional HTP behaves similarly to a conventional planar lifting surface (placed in the downwash of the main wing) and therefore its behaviour is sufficiently well known and modelled today. In the case of a V-tail design with a dihedral angle close to 45°, the development of the drag due to trim is expected to be more complex.

To investigate the development of the trim drag in the case of the V-tail configuration, RANS calculations have been carried out and analysed with the

ONERA far-field drag extraction tool for different tail settings ranging from $i_H=0^o$ to $i_H=-2.8^o$. All calculations have been performed at the same lift condition of $C_L=0.4$, representative of a cruise condition at fixed aircraft weight. Each calculation therefore yields a different trim condition, i.e. a different location of the CG of the aircraft. Special effort has been made to generate hybrid CFD meshes of good quality in the region of the tail wake as illustrated in Figure 4. The V-tail meshes comprises about 5.7 millions cells and includes a block of hexahedral cells downstream of the tail. In order to derive the trim drag due to the tail lift, a calculation has also been made for the tail-off aircraft configuration in the same lift condition of $C_L=0.4$.

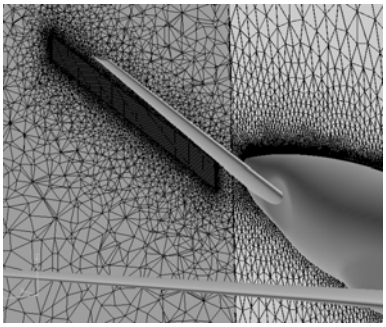

Figure 4: View of some mesh refinements included in the hybrid meshes to properly capture the tail wake.

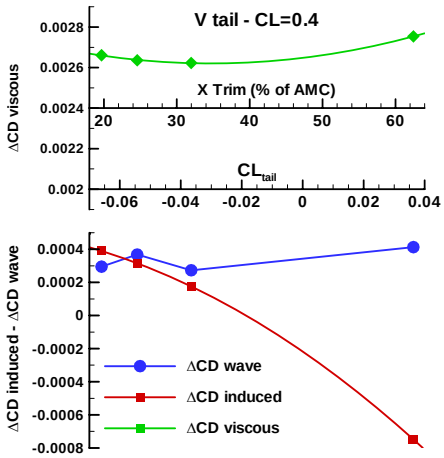

Figure 5: Evolution of the different V-tail viscous, wave and induced drag components with the tail lift (or location of aircraft CG).

The application of the far-field drag extraction technique provides a breakdown of the total drag into its viscous (friction + viscous pressure drag), wave and lift-induced components for each configuration. "Tail drag" and its different components are then defined with respect to the tail-off configuration as follows:

$$\Delta CD_X = CD_X^{Vtail} - CD_X^{Tail-off}, \qquad (3)$$

with "*X*" representing any of the total/viscous/wave/induced drag components. The evolution of the different "tail drag" components with the location of the aircraft CG is plotted in Figure 5. Compared to the tail-off configuration, the main source of drag increase is of course the viscous drag component, explained by an 11% increase in wetted surface area. The variation of this viscous components is however limited to a specific trim condition. The lift-induced drag component exhibits the largest variations, with a 4% forward displacement of the CG resulting in a 1 drag count increase. It should be noted that for positive tail lift

conditions (high tail setting angle), the V-tail aircraft has a lower lift-induced drag (negative value of $\Delta CD_{induced}$).

Finally, the wave drag term contributes only very little to the total "tail drag" (Figure 5) and shows very small variations with a change in trim condition (about 1 drag count). The localisation of the flow regions contributing to the wave drag is is also possible by means of the far-field analysis. The streamwise wave drag distribution for the V-tail aircraft at C_L=0.4 and at three tail settings is given in Figure 6. This shows that for the highest tail setting (i_H=0°) at which the tail has a positive lift contribution, the tail itself contributes to the total wave drag at about the same level as the wing. In contrast, the tail does not noticeably contribute to the total wave drag by itself for the more negative tail settings, although it affects the wave drag produced on the wing, which can be explained by a higher wing lift required to compensate the higher negative tail lift.

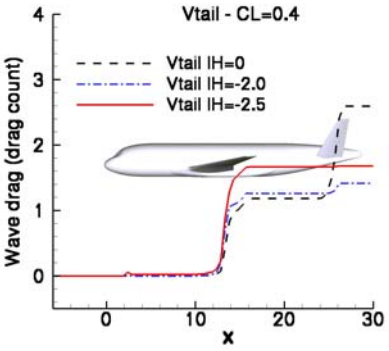

Figure 6: Streamwise wave drag development (accumulated) for the V-tail configuration at C_L=0.4 and 3 tail settings

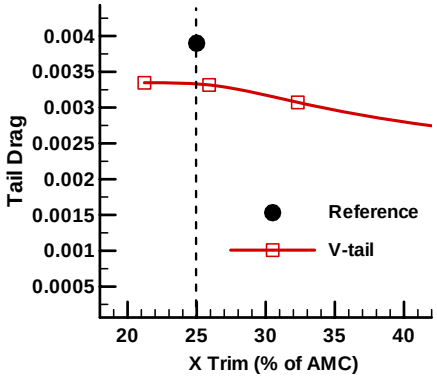

Figure 7 : Comparison of reference and V-tail drag at C_L=0.4 for a CG placed at 25% of the Mean Aerodynamic Chord.

6 Cruise Drag Comparison

Using the far-field drag analysis technique, accurate evaluations of the total drag for the V-tail and the reference tail configuration have been performed. The results obtained are given in Figure 7 which provides a comparison of the "tail drag" for the V-tail and the reference tail design at C_L=0.4. For the trim condition corresponding to a CG located at 25% of the mean aerodynamic chord (which is the only trim condition evaluated for the aircraft with reference tail), the V-tail design offers a 15% reduction of the tail drag.

7 Conclusion

The cooperative ONERA-DLR research effort conducted within the NEFA project as presented in this paper provides insight into the aerodynamics of alternative tail

types, a subject for which little recent data is available. The results of the CFD investigations at cruise conditions and wind tunnel Reynolds numbers clearly prove the drag reduction potential of the V-tail, which more than offsets its lower efficiency. As installation and control surface redundancy issues could be resolved through the work of other partners within NEFA, and weight estimation with high-fidelity tools in other work packages showing no weight penalty for the V-tail, this tail type seems to be the premier choice for the tail configuration of a highly efficient, low drag and therefore low-fuel consumption and low-emission aircraft. While it was shown that the U-tail does not offer any drag reduction potential, it also became clear that its performance is no worse than that of a conventional tail. It may therefore be used if more emphasis is put on other aspects of the aircraft design like shielding of the noise of aft fuselage-mounted engines. The results as presented will therefore help to evaluate the potential contribution of novel empennage types to achieve the goals set forth in the European Vision 2020 for future civil transport aircraft with regard to reduced environmental impact of air traffic.

Acknowledgements

The work was performed under the European Research Contract No. G4RD-CT-2002-00864 as part of the 5th framework programme "Competitive and Sustainable Growth". The authors would like to thank the European Commission for supporting this pre-competitive research work.

References

[1] T. Gerhold: "Overview of the Hybrid RANS Code TAU", *Notes on Numerical Fluid Mechanics*, edited by N. Kroll and J. Fassbender, Vol. 89, Springer 2005, pp. 81-92

[2] D. Destarac: "Far-Field/Near-Field Drag Balance and Application of Drag Extraction in CFD", VKI Lecture Series 2003, CFD-based Aircraft Drag Prediction and Reduction, National Institute of Aerospace, Hampton (VA), November 3-7, 2003.

[3] J. Van Der Vooren and D. Destarac: "Drag-Thrust analysis of a Jet-propelled Transonic Transport Aircraft; Definition of Physical Drag Components, Submitted for publication, November 2002.

[4] Centaur Mesh Generator, CentaurSoft, URL: http://www.centaursoft.com/ [cited May 2005]

[5] J. Wild: "AeroForce – Thrust/Drag Bookkeeping and Aerodynamic Force Breakdown over Components". DLR IB 129-99/9, DLR, Braunschweig, 28 June 1999

[6] Brodersen, O., et. al.: "Aerodynamics Investigations in the European Project ROSAS (Research on Silent Aircraft Concepts)", AIAA Paper 2005-4891, accepted for presentation at the 23rd AIAA Applied Aerodynamics Conference, 6 - 9 June 2005, Toronto, Canada